ResearchGate

See discussions, stats, and author profiles for this publication at: https://www.researchgate.net/publication/231291330

Adsorption-Partitioning Uptake of Nine Low-Polarity Organic Chemicals on a Natural Sorbent

ARTICLE *in* ENVIRONMENTAL SCIENCE AND TECHNOLOGY · DECEMBER 1998

Impact Factor: 5.33 · DOI: 10.1021/es980581g

CITATIONS
230

READS
65

2 AUTHORS, INCLUDING:

William P Ball
Johns Hopkins University
133 PUBLICATIONS **4,463** CITATIONS

SEE PROFILE

Available from: William P Ball
Retrieved on: 03 February 2016

Environ. Sci. Technol. **1999**, *33,* 262−269

Adsorption-Partitioning Uptake of Nine Low-Polarity Organic Chemicals on a Natural Sorbent

GUOSHOU XIA AND WILLIAM P. BALL*

Department of Geography and Environmental Engineering, The Johns Hopkins University, 3400 North Charles Street, Baltimore, Maryland 21218

Sorption of comparatively nonpolar organic chemicals by natural solids not only can be predominated by partitioning with organic matter but also can reflect a substantial contribution from adsorption at low relative concentration. Sorption of nine polycyclic aromatic hydrocarbons (PAHs) and chlorinated benzenes (CBs) was investigated on a subsurface aquitard through batch study, with results interpreted by a composite adsorption-partitioning model. For both PAHs and CBs, the low-concentration adsorption slope and the coefficient for partitioning each correlated well with K_{ow}; however, PAHs consistently sorbed more strongly than CBs at given K_{ow}. For all chemicals, adsorption contributions were only important at low relative concentration and could be successfully modeled by assuming either Langmuir-type or Polanyi-type isotherms. Isotherms for all liquid chemicals fell on a single isotherm when plotted on a Polanyi basis (adsorbed volume per mass of sorbent versus adsorption potential density), providing evidence that a pore-filling phenomenon is involved. Adsorbed volumes of solid chemicals were observed to be less than those of liquids at the same adsorption potential density, consistent with a reduction in packing efficiency and as previously reported for activated carbons. These results suggest that the adsorption contribution is from pore filling within microporous solids.

Introduction

Sorption of low-polarity and nonpolar organic chemicals (NOCs) by natural subsurface solids or aquatic sediments can be predominated by partitioning of dissolved solute between water and naturally occurring organic matter (*1*−*6*). Nonetheless, many studies have found that sorption isotherms for such systems can show substantial deviations from a linear partition model, especially when very low concentrations of the NOCs are studied and/or shales or other sources of diagenetically altered organic matter are present (*7*−*9*). In such systems, order-of-magnitude variations in aqueous concentration are commonly considered, with data plotted on logarithmic axes and the Freundlich isotherm equation used to model the results. This equation takes the following form:

$$q_e = K_F C_e^{1/n} \quad (1)$$

Here C_e is the aqueous equilibrium concentration (mg/mL), q_e is the corresponding sorbed concentration (mg/g), and K_F and $1/n$ are adjustable parameters used to fit the model to data. In systems of NOCs with natural sorbents, $1/n$ is almost always found to have a value less than or equal to 1.

Several groups of investigators have postulated that natural sorbents may comprise two principal types of heterogeneous sorption domains, one of which is a medium for NOC dissolution (partitioning), and the other of which contains surfaces or "sites" for NOC adsorption (*7*−*12*). A "distributed reactivity" model or simplified dual-mode model has been proposed to separately account for solute distribution among the different sorption domains (*7, 10, 11, 13, 14*). In these models, a Langmuir-type equation has been commonly used to fit the nonlinear adsorption component. The overall adsorption-partitioning model takes the following form when a single type of "site" for Langmuir adsorption is assumed:

$$q_e = \frac{Q_{max} b C_e}{1 + b C_e} + K_p C_e \quad (2)$$

In this model, Q_{max} is the adsorption capacity (mg/g), $Q_{max}b$ is the isotherm slope in the low concentration (Henry's Law) range (mL/g), and K_p is the coefficient for partitioning with a bulk organic phase (mL/g).

Although many of the assumptions of a Langmuir model (*15*) are likely not met in natural systems, postulation of multiple "site types" allows simulation of a wide range of sorption data, in a similar manner as the Freundlich isotherm. Some principal differences from the Freundlich approach are that Langmuir-type modeling reverts to linearity at very low aqueous concentration and that Langmuir-type models have a maximum capacity for adsorption, even when multiple "site types" are assumed. In the work presented here, we include analysis of our results by a Langmuir-type adsorption-partitioning model of the form of eq 2, primarily as a mathematical means of quantifying the implied "monolayer capacity" for such a model and for defining a "best-fit" low-concentration slope. In these contexts, we limit ourselves to the single-site Langmuir model.

One conceptual difficulty of the Langmuir-type model is that, in some cases, the estimated adsorption capacity exceeds greatly the theoretically allowed monolayer coverage on soil organic matter (SOM) surfaces (*10*). Although adsorption on nitrogen-inaccessible internal SOM surfaces has been proposed to account for this (*16*−*19*), there is no direct evidence for such a phenomenon. Moreover, very high-energy adsorption of NOCs from aqueous solution may be unlikely in a "typical" SOM phase dominated by polar humic substances. In studies with a peat soil, lower adsorbed mass has been observed for relatively larger sorbates, such as phenanthrene (*13*) and atrazine (*10*), relative to 1,3-dichlorobenzene or trichloroethene (*10*). Whereas some investigators have taken these results to indicate that large sorbates may be excluded from adsorption internal to the SOM matrix (*16*−*19*), there is no direct evidence for the existence of nitrogen-inaccessible but compound-specific internal voids, as mentioned before. In the current work, we offer an alternative explanation for low adsorbed volume of such solid sorbates, supported by Polanyi-based modeling.

More specifically, if we postulate the presence of an adsorption domain comprised of microporous nonpolar surfaces, then pore-filling is likely and a Langmuir-type modeling approach lacks mechanistic basis. The presence of such microporous domains is consistent with the results of Chiou and Kile (*9*), who have suggested that low concentration adsorption is associated with high-surface-area

* Corresponding author phone: (410)516-5434; fax: (410)516-8996; e-mail: bball@jhu.edu.

10.1021/es980581g CCC: $18.00 © 1999 American Chemical Society
Published on Web 12/05/1998

carbonaceous materials (HSACM). Examples of such materials are charcoal-like particles from biomass burning (*9, 20*) or other forms of carbon black (*21*) that undoubtedly exist in many (if not most) soils and sediments, albeit at low concentration. We speculate that HSACM could also be associated with oil shales and other rocks that contain kerogen-based organic matter. For example, microporous regions and hydrophobic surfaces may be associated with the ultrathin (10−30 nm) kerogen laminae that are believed to derive from nonhydrolyzable fractions of microalgae (*22*).

Adsorption of low-polarity organic chemicals to HSACM is likely to be nonspecific and may occur in a similar manner as with activated carbon (*9*). For adsorption of this type, Polanyi adsorption theory has been successfully applied by Manes and co-workers (*23*−*30*) as well as by other researchers (*31*−*33*), including applications to both gas adsorption and to adsorption from aqueous solution. Aqueous solution application was first proposed by Wohleber and Manes (*24, 34*), and Manes and co-workers have also developed the concepts of solid adsorbate packing (*25*−*27, 30*) which we discuss subsequently. The overall theory is hereafter referred to as a Polanyi−Manes modeling approach.

The Polanyi adsorption theory may be summarized as follows: for a given adsorbate molecule at any point in the neighborhood of an adsorbent surface there exists an adsorption potential (ϵ) that depends on proximity to the surface and the nature of the adsorbate. Locations with the same value of ϵ form equipotential surfaces that together with the solid surface enclose a volume $V(\epsilon)$. In terms of adsorbed volumes of sorbates, plots of $V(\epsilon)$ against ϵ will form a "characteristic" adsorption curve that, for a nonspecifically interacting adsorbate, will be determined by the structure of the adsorbent. For adsorption of partially miscible solutes from aqueous solution, the effective adsorption potential (ϵ_{sw}, cal/mol) can be defined as

$$\epsilon_{sw} = RT \ln(S_w/C_e) \tag{3}$$

in which S_w and C_e are the solubility and the equilibrium concentration of the solute at temperature T (K), respectively, and R is the ideal gas constant. The critical difference between vapor-phase and solution-phase adsorption is that adsorption from aqueous solution has to replace an equal volume of water (*30*). The net adsorption potential of solutes is

$$\epsilon_{sw} = RT \ln(S_w/C_e) = \epsilon_s - V_s(\epsilon_w/V_w) \tag{4}$$

Here, V_s and V_w are the molar volumes (cm^3/mol) of solute and water, respectively, and ϵ_s and ϵ_w are the adsorption potential (cal/mol) of solute and water, respectively. In the case of NOC adsorption from aqueous solution onto nonpolar carbon surfaces, ϵ_w/V_w can reasonably be assumed to have an approximately constant value, with a reported average value of $0.28 \times \epsilon_s/V_s$ for hydrocarbons at the same adsorbed volume (*24*). For such surfaces, we therefore expect ϵ_{sw} to be proportional to ϵ_s. Moreover, if adsorption is nonspecific—i.e., if similar mechanisms of adsorption apply to all sorbates considered—then we expect ϵ_{sw} to be a function only of adsorbed volume. A complication to the above situation occurs for the case of sorbates which are normally solids at the temperatures of adsorption. Manes and co-workers (*25*−*27, 30*) have studied the adsorption of such sorbates from liquid solution and have observed that they pack less efficiently than chemicals which will condense into liquids. For example, Chiou and Manes (*26*) determined the adsorption from water of several chemicals that melt under water at moderately elevated temperature. In all cases, an increase in adsorption temperature produced a constant and discontinuous jump in adsorption (for given relative concentration) at temperature corresponding to the underwater melting point. The difference is attributed to inefficient packing of the presumably solid-phase adsorbate, which is believed to result from structural incompatibility between the crystal structure of the solid and the adsorbent pore dimensions (*25, 26, 30*). By contrast, we expect complete pore filling when sorbates are present in a liquid state.

Polanyi proposed no theoretical equation for predicting the relationship between the adsorbed volume against the equilibrium adsorption potential. However, Dubinin (*35*) suggested that a plot of adsorbate volume against adsorption potential density (adsorption potential divided by sorbate molar volume) would yield similar curves (later called "correlation curves") for a wide variety of adsorbates. For activated carbons, Crittenden and co-workers (*33*) suggested the following empirically derived relation between adsorbed volume and adsorption potential (ϵ)

$$\log(q_e') = \log(Q_o') + a'(\epsilon_{sw}/V_s)^{b'} \tag{5}$$

in which, q_e' is the adsorbed solute volume per unit mass of sorbent (cm^3/kg), Q_o' is the adsorption volume capacity at saturation (cm^3/kg), and a' and b' are fitting parameters. Here, we use q_e' and Q_o' for adsorbed volume in order to differentiate from definitions based on adsorbed solute mass (q_e and Q_o).

For a given sorbent, the sorption isotherm of adsorbed volume per unit mass of sorbent versus the adsorption potential density is expected to fall on a single line for all liquid sorbates if there are no specific interactions between sorbates and the sorbent surface (*30*). For the case of relatively nonpolar organic sorbates adsorbing from aqueous solution, any specific polar interactions with adsorption surfaces will tend to be weak and will be swamped out by water (*24*). For these reasons, it has been commonly observed that the maximum adsorbate volume for hydrocarbons on carbon surfaces tends to be the same for all liquids and condensed vapors (*30*). By contrast, if sorbates are solids in the adsorbed state, then the adsorption capacity should be less than that for liquids, for reasons previously noted.

The following equation describes an overall adsorption-partitioning model for which the adsorption term is described by a Polanyi−Manes type of modeling approach:

$$q_e = Q_o' \times 10^{a'(\epsilon_{sw}/V_s)^{b'}} \times \rho + K_p C_e \tag{6}$$

Here, ρ is the molecular density (g/cm^3).

In this study, we describe our investigation of the sorption behavior of two groups of organic chemicals, namely polycyclic aromatic hydrocarbons (PAHs) and chlorinated benzenes (CBs). We did not include strongly polar or ionizable chemicals in our study since these sorbates would be subject to additional specific adsorption phenomena not applicable to NOCs. All studies were conducted with a natural geosorbent comprising fine-grained material taken from an aquitard at Dover Air Force Base, DE. A composite adsorption-partitioning model is used to interpret the observed sorption behavior, with adsorption component results interpreted in the context of both Langmuir-type modeling (eq 2) and the Polanyi−Manes approach (eq 6). To our knowledge, this is the first application of Polanyi-based isotherms to describe NOC uptake by natural solids (geosorbents). The application of the isotherm modeling to the data sheds light on the nature of the sorption process with the material studied. Moreover, we believe that both the overall and Polanyi-based modeling approaches may have broad applicability for describing NOC uptake by natural sorbents.

Experimental Section

Materials. The sorbent studied is an aquitard material from an upper confining unit to the Calvert Formation in the

TABLE 1. Selected Physicochemical Properties of the Chemicals Used in Sorption Experiments

chemical	abbr	MW (g/mol)	T_m (°C)	density (g/cm^3)	log (K_{ow})	S_w (mg/L)	molar volume[a] (cm^3/mol)
benzene	Benz	78.1	5.5	0.877	2.13 (*43*)	1800 (*44*)	89
chlorobenzene	CB	112.6	−45.6	1.106	2.92 (*43*)	500 (*1*)	102
1,2-dichlorobenzene	DCB	147.2	−17.0	1.305	3.38 (*43*)	125 (*43*)	113
1,2,4-trichlorobenzene	TCB	181.5	16.9	1.454	4.05 (*6*)	35 (*1*)	125
1,2,4,5-tetrachlorobenzene	TeCB	215.9	140.0	1.858	4.50 (*45*)	0.6 (*1*)	116.2
naphthalene	Naph	128.2	80.6	1.16	3.30 (*43*)	31.7 (*1*)	110.5
fluorene	Fluo	166.2	113.0	1.20	4.18 (*43*)	1.82 (*43*)	138.5
phenanthrene	Phen	178.2	99.5	1.17	4.57 (*43*)	1.29 (*1*)	152.3
pyrene	Pyre	202.3	156.0	1.27	5.13 (*43*)	0.135 (*1*)	159.3

[a] Molar volume is estimated as the ratio of molecular weight and the density.

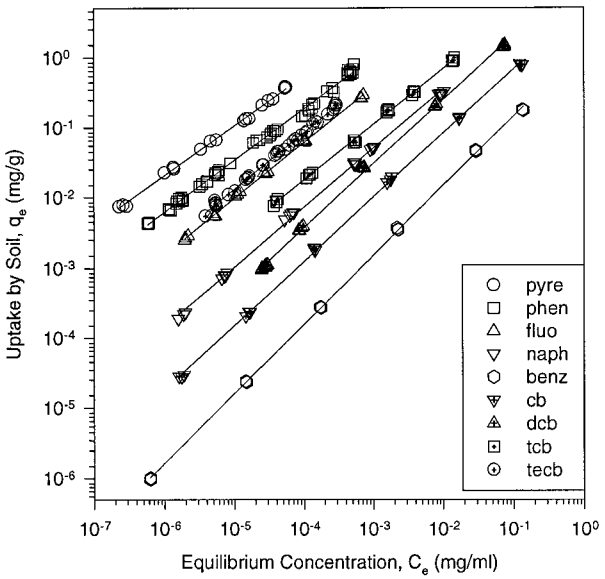

FIGURE 1. Sorption isotherms of nine chemicals with Dover DGSL.

Delaware coastal plain, tentatively identified as the Choptank Formation and believed to date to the middle to late Miocene (*36*). Material was collected from four soil cores taken from approximately 14.6−15.2 m below ground surface at Dover Air Force Base, DE, and has been previously identified as "dark gray silt loam (DGSL)" (*37*). The details for sample collection have been described elsewhere (*37*). After collection, the material was carefully air-dried under aluminum foil cover in a large stainless steel container, homogenized, and riffle-split to fractions of about 200 g each. Particle size analysis (*38*) indicated that this material contains 17% sand, 65% silt, and 18% clay. Total carbon content was measured by a high-temperature combustion method (*37*) to be 1.49% with no measurable carbonate content. Surface area was measured by multiple point nitrogen BET to be 4.0 m^2/g.

The nine organic chemicals studied were benzene (Benz), naphthalene (Naph), fluorene (Fluo), phenanthrene (Phen), pyrene (Pyre), chlorobenzene (CB), 1,2-dichlorobenzene (DCB), 1,2,4-trichlorobenzene (TCB), and 1,2,4,5-tetrachlorobenzene (TeCB). All chemicals were obtained from Sigma-Aldrich Chemical Co. (St. Louis, MO). The radiochemical purities and specific activities are Benz 99+%, 12.7 mCi/mmol; Naph 99+% in methanol solution, 49.8 mCi/mmol; Fluo 99+%, 14.55 mCi/mmol, 0.7 mCi/mL in toluene solution; Phen 98%, 13.3 mCi/mmol; Pyre 99+%, 58.7 mCi/mmol, 1.0 mCi/mL in toluene solution; CB 99+%, 12.8 mCi/mmol; DCB 99+%, 2.2 mCi/mmol; TCB 99+%, 1.6 mCi/mmol; and TeCB 98%, 3.7 mCi/mmol. All radiochemicals were used as received. Chemicals in unlabeled forms had purity higher than 99% and were used as received. The selected physicochemical properties of these chemicals are given in Table 1. Spike solutions were prepared in methanol. For chemicals received in methanol, the mole fraction of methanol in all samples was held to below 10^{-3} and therefore below a level that should influence aqueous activity of the sorbates (*39*). For Fluo and Pyre, the final toluene concentration in sorption samples was less than 0.1 mg/L. Separately conducted binary adsorption experiments (*40*) indicate that the competitive effect of toluene on sorbed concentration (q_e) of Fluo and Pyre should be less than 3% and 1%, at the lowest evaluated concentrations of Fluo and Pyre, with much smaller effects at higher concentration. For all compounds, ^{14}C activity of spike solutions and water samples was determined by injection into liquid scintillation fluid, followed by counting (Model LS3801, Beckman Instruments, Fullerton, CA).

TABLE 2. Fitted Parameters of Observed Sorption Data by Freundlich Isotherm

NOC	N[a]	K_f[b]	$1/n$[b]	r^2	MWSE[c]
Benz	18	1.62 ± 0.045[d]	1.00 ± 0.012	0.9999	0.0127
CB	18	5.36 ± 0.37	0.91 ± 0.010	0.9996	0.0065
DCB	25	14.6 ± 1.50	0.90 ± 0.007	0.9983	0.0112
TCB	24	25.8 ± 2.11	0.80 ± 0.008	0.9988	0.0041
TeCB	36	128.2 ± 5.92	0.80 ± 0.010	0.9976	0.0043
Naph	30	18.3 ± 1.11	0.85 ± 0.005	0.9977	0.0064
Fluo	18	98.1 ± 0.42	0.80 ± 0.007	0.9983	0.0026
Phen	53	169.8 ± 11.04	0.74 ± 0.014	0.9970	0.0092
Pyre	18	374.1 ± 16.58	0.71 ± 0.014	0.9976	0.0045

[a] N = number of observations. [b] Parameters of Freundlich isotherm equation: $q_e = K_F C_e^{1/n}$; units on K_F are (mg/g)/(mg/mL)$^{1/n}$. [c] MWSE = mean weighted square error = $1/\nu\sum[(q_{measd} - q_{model})^2]/q^2_{measd}$ where ν is the number of degrees of freedom; here, $\nu = N - 2$). [d] Mean ± standard deviation.

Sorption Experiments. Sorption experiments were conducted in glass centrifuge tubes with aluminum foil facing added to the inside of PTFE-lined solid phenolic screw caps. Tubes were 10 mL for all experiments except for pyrene, for which 50 mL tubes were used in order to maintain reasonable sorbent mass (>0.01 g) at the high liquid:solid ratios required. A total of 0.01 to 2.5 g of soil, followed by synthetic groundwater containing 0.005 M $CaCl_2$ and 0.02% NaN_3 (by weight), was added to the preweighed glass centrifuge tubes. Air bubbles were removed by completely mixing the soil suspensions for 3 min and allowing tubes to sit overnight before final filling and spiking. Three to 8 μL of stock solution was added immediately prior to sealing, and the ^{14}C activity spiked was carefully monitored through periodic direct injections into scintillation fluid. The sorption tubes were mixed end-over-end at 2 rpm for 7 days at room temperature (22 ± 1 °C). Preliminary experiments with sorption times up to 70 days had indicated that less than 3 days were required to achieve approximate (apparent) equilibrium conditions for Phen and Naph with this fine-grained material. In this regard, our experiments do not specifically address the potential for a small but perhaps important fraction of

TABLE 3. Fitted Parameters of Observed Sorption Data by Adsorption-Partitioning Model with Langmuir-Type Equation for Adsorption Component

NOC	N^a	K_p (mL/g)	$\log(K_{oc})^b$	Q_{max} (mg/g)	$b \times 10^{-3}$ (mL/mg)	MWSE[c]	$(1/b)/S_w)^d$
Benz	18	0.90 ± 0.039[e]	1.78	0.1134 ± 0.0089	0.007 ± 0.00081	0.0037	0.079
CB	18	5.62 ± 0.17	2.58	0.076 ± 0.024	0.073 ± 0.032	0.0374	0.027
DCB	25	18.2 ± 0.26	3.09	0.104 ± 0.017	0.202 ± 0.0487	0.0012	0.040
TCB	24	56.4 ± 1.90	3.58	0.137 ± 0.024	0.780 ± 0.193	0.0198	0.037
TeCB	36	626.6 ± 17.8	4.62	0.0249 ± 0.004	39.9 ± 1.97	0.0029	0.042
Naph	30	29.5 ± 0.42	3.30	0.0294 ± 0.003	2.25 ± 0.417	0.0107	0.014
Fluo	18	346.8 ± 10.0	4.37	0.0412 ± 0.006	18.6 ± 3.84	0.0091	0.029
Phen	53	1235 ± 24.8	4.92	0.0469 ± 0.006	101.6 ± 23.2	0.0093	0.008
Pyre	18	6115 ± 147.6	5.61	0.0462 ± 0.005	528.3 ± 106	0.0038	0.014

[a] N = number of observations. [b] K_{oc}, soil organic carbon normalized partitioning coefficient (mL/g). [c] MWSE as defined in Table 2; here, $\nu = N - 3$. [d] Value of C_e/S_w at which the Langmuir-modeled contribution to sorption would equal 50% of Q_{max}. [e] Mean ± standard deviation.

sorption that may be much slower to reach equilibrium (i.e., a fraction with equilibration times much greater than 70 days).

After the completion of each experiment, the samples were centrifuged at 2500 rpm (about 550 g) for 30 min, and about 1−2 mL of supernatant was taken for scintillation counting. Twelve to 20 blank samples (without soil) were included in each set of sorption isotherm experiments. These were used to directly account for losses by assuming mass losses proportional to the final aqueous concentrations (*39*). Solute losses to headspace, glass wall, aluminum foil, and caps in blank samples (without soil) were less than 4% for all test solutes conducted in 10 mL centrifuge tubes, although roughly 6% loss was observed in the system of pyrene in 50 mL centrifuge tubes.

Results and Discussion

Sorption Results. Sorption isotherms for all nine chemicals are shown in Figure 1, together with fitted Freundlich isotherms. The parameters for the isotherms are summarized in Table 2, together with the calculated mean weighted square error (MWSE; (*39*)), defined as described in the table footnote. Except for that of benzene, all isotherms exhibit Freundlich exponents less than one. The less soluble NOCs were more strongly sorbed at all concentrations but especially so at the lower concentrations. This is reflected in the tabulated values of the Freundlich exponents, which are increasingly below 1.0 for the less soluble NOCs. As shown in Table 2, Freundlich exponents as low as 0.71 and 0.74 were obtained for the two most hydrophobic chemicals (pyrene and phenanthrene).

Composite Adsorption-Partitioning with Langmuir-Type Modeling Approach. Initially, and as previously used by others (*13, 16*), a Langmuir-type equation was assumed for the adsorption component. The overall adsorption-partitioning model has been given in eq 2. Fitted parameters for this modeling included the nonlinear adsorption capacity (Q_{max}), the partitioning coefficient (K_p), and the Langmuir-type equation parameter (b) for each solute, as shown in Table 3. Fitting was based on a weighted least squares minimization, with MWSE results as also shown in the table.

We note that our experimental systems were not sufficiently sensitive to provide very accurate estimation of Q_{max}. More specifically, because the sorption data in the concentration range of the adsorption plateau were dominated by partitioning, estimates of adsorption in this region represent small differences of two large numbers. This is apparent from our plots of total and adsorbed concentrations, as shown in Figure 2 (discussed subsequently). It was especially difficult to estimate the Langmuir modeling parameters accurately for benzene and chlorobenzene, for which overall sorption behavior was dominated by partitioning over a large fraction of the observed concentrations. Nonetheless, we are able to note that the results of Table 3 show a general trend of higher Q_{max} for liquid chemicals than for those chemicals which are solid at the test temperature (last five rows of Table 3). As previously described, others (*10, 16−19*) have suggested that higher Q_{max} for smaller organic molecules may be the result of adsorption interior to humified SOM. For the chemicals studied here, however, some chemicals do not follow a simple size trend. For example, the molar volume of 1,2-DCB is similar to those of 1,2,4,5-TeCB and Naph; however, the adsorption capacity for 1,2-DCB is much higher. Later in this paper, we explore the possibility that the adsorption may take place in micropores of HSACM. In this case, differences in adsorption capacity among solid and liquid adsorbates are an expected result, accounted through differences in packing efficiency.

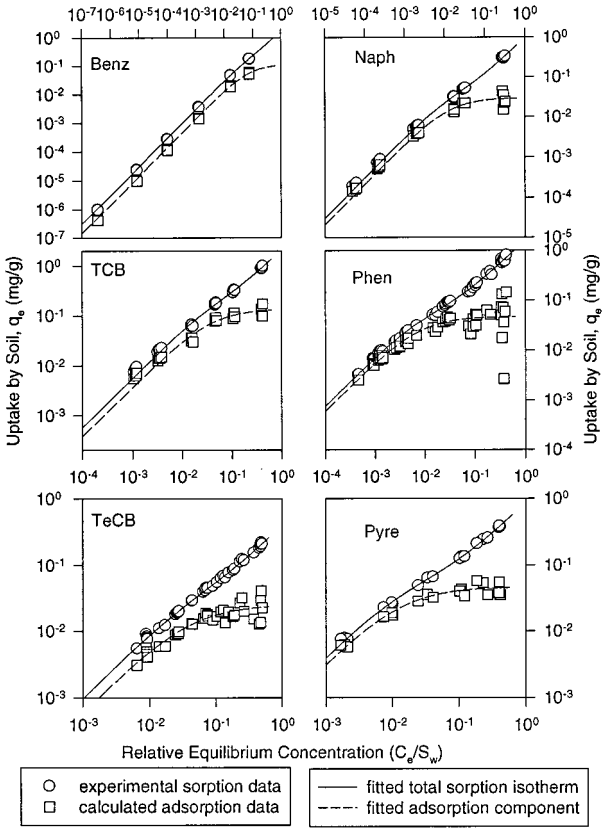

FIGURE 2. Representative composite adsorption-partitioning isotherms with Langmuir-type equation for adsorption component.

Representative examples of the Langmuir-type fit as applied to experimental sorption data are shown in Figure 2 for six representative chemicals. Also shown is the calculated adsorption component after subtraction of the estimated partitioning contribution as well as the fitted lines from the

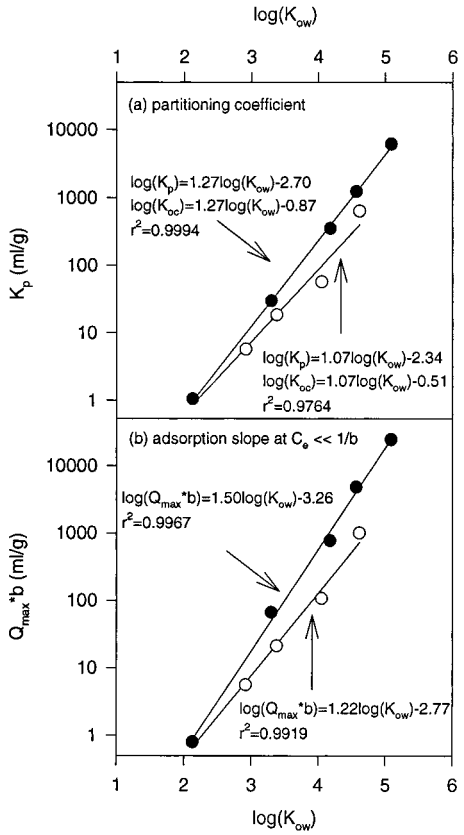

FIGURE 3. Relationship between partitioning coefficient, the adsorption slope at $C_e \ll 1/b$ and octanol−water distribution coefficient (open circles are for CBs and solid circles are for PAHs).

composite adsorption-partitioning model. In general, the fitted lines are in good agreement with both the overall sorption data and the estimated adsorption component. For the overall (observed) sorption, both the model lines and the experimental data follow a subtle but interesting curvature on this log−log plot, with approximately linear behavior (slope of one) at low relative concentration, followed by a slightly lower slope that transitions to another region of sorption linearity at high relative concentrations. Such linearity of sorption in the high concentration region has been previously emphasized by others (*9*). The ability to simulate such behavior represents an important distinction of the current modeling approach from the Freundlich model. In terms of the overall goodness of fit, however, there is no clear distinction among the two models—the composite model exhibits substantially lower MWSE values for only four of the nine chemicals. This may reflect a better ability of the Freundlich model to capture adsorption heterogeneity in the low concentration region for some systems. On the other hand, readers should note that we have comparatively few data in the linear (high concentration) region of sorption. Also, the dominance of partitioning in these systems prevents us from making precise estimates of adsorbed concentrations (for reasons previously cited). Therefore, we are reluctant to discriminate among these models based solely on "goodness of fit" criteria.

Correlation of Sorption with Log(K_{ow}). Figure 3a,b shows correlation of log(K_p) and log($Q_{max}b$) with log(K_{ow}), respectively, for all nine chemicals. It is clear that both the partitioning slope (K_p) and the low-concentration (Henry's Law region) isotherm slope ($Q_{max}b$) are well correlated with K_{ow} in a manner consistent with linear free energy relationships. The data may imply that differences in K_{ow}, K_p, and low-concentration adsorption are all controlled primarily by solubility and molecular size for these chemicals. Although

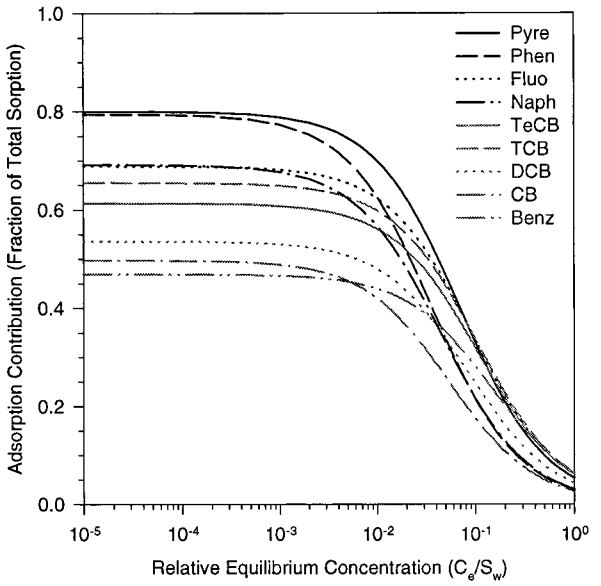

FIGURE 4. Contribution of adsorption component to the overall sorption as a function of relative concentration.

the above definition of a low-concentration isotherm slope is specific to the assumed Langmuir-type of modeling, plots of dq_{ad}/dC_e under the Polanyi−Manes model (eq 6) show a similar trend when applied to low concentration results (*40*). With this model, and as shown subsequently, adsorption differences among the liquid sorbates are fully accounted in terms of sorbate solublity and molar volume.

Also shown in Figure 3a are the correlation equations in terms of K_{oc} (= K_p/f_{oc}, where f_{oc} = 0.0149). Our correlation coefficients for CBs (slope = 1.07, intercept = −0.51) are roughly similar to the results of Karickhoff (slope = 1.00, intercept = −0.21) (*1*); however, the slope and the intercept coefficients for PAHs are somewhat higher and lower, respectively. Interestingly, log(K_{oc}) values for DCB, Naph, Phen, and Pyre are higher than those reported by Chiou and co-workers (*41, 42*) for sediments and soils by 0.2−0.6 log units and 0.5−0.8 log units, respectively. These results suggest that the silt loam from this aquitard environment contains an organic matter phase for partitioning that is more nonpolar than that found in the "normal" surface soils and sediments studied by those investigators. We speculate that the comparatively nonpolar nature of the NOM may reflect the nature and history of the organic matter in the aquitard, which is a depositional formation of the ancient Delaware Bay (*36*), and may have been subjected to anoxic conditions for much (if not all) of its history.

K_p and $Q_{max}b$ values of Table 3 show that, at a given K_{ow}, PAHs are more strongly sorbed than CBs in the contexts of both the partitioning and low-concentration isotherm slope. The differences among these two chemical groups decrease with decreasing log(K_{ow}) and vanish at benzene. Similar differences between PAHs and CBs have been observed by Chiou et al. (*41*), who suggest that stronger partitioning of PAHs can be a result of their more compatible cohesive energy densities with aromatic components of the NOM.

Comparison of Figure 3 (parts a and b) shows that, for both PAHs and CBs, the increase of the very low concentration isotherm slope ($Q_{max}b$) has a stronger dependence on log(K_{ow}) than does the partition coefficient, to the point that $Q_{max}b$ values are substantially greater than K_p for the more hydrophobic chemicals. This result implies that the adsorption surfaces have a low affinity for water (relative to their affinity for nonpolar HOCs) and is also the reason more hydrophobic NOCs are more heavily influenced by adsorption. This is clearly illustrated by Figure 4, which shows the

TABLE 4. Fitted Parameters of Observed Sorption Data by Adsorption-Partitioning Model with Polanyi Adsorption Theory for Adsorption Component

NOC	N^a	K_p (mL/g)	log(K_{oc})^b	Q_o' (cm^3/kg)	Q_o (mg/g)	a'	b'	MWSE^c	packing efficiency^d
Benz	18	1.26 ± 0.04^e	1.93	0.103 ± 0.0014	0.0904 ± 0.0012	$-1.06 \times 10^{-2} \pm 1.26 \times 10^{-4}$	1.378 ± 0.044	0.0085	
CB	18	5.68 ± 0.31	2.58	0.125 ± 0.0031	0.1382 ± 0.0034	$-3.44 \times 10^{-3} \pm 1.38 \times 10^{-4}$	1.657 ± 0.041	0.0301	
DCB	25	16.71 ± 1.51	3.05	0.163 ± 0.0013	0.1803 ± 0.0168	$-7.08 \times 10^{-3} \pm 1.30 \times 10^{-3}$	1.557 ± 0.032	0.0011	
TCB	24	52.24 ± 2.63	3.54	0.141 ± 0.0060	0.2047 ± 0.0087	$-4.64 \times 10^{-3} \pm 3.29 \times 10^{-4}$	1.685 ± 0.077	0.0077	
TeCB	36	566.4 ± 46.8	4.58	0.022 ± 0.0008	0.0409 ± 0.0146	$-6.07 \times 10^{-3} \pm 3.74 \times 10^{-4}$	1.585 ± 0.008	0.0032	0.16
Naph	30	29.4 ± 2.83	3.30	0.023 ± 0.0050	0.0267 ± 0.0058	$-1.17 \times 10^{-4} \pm 1.06 \times 10^{-5}$	2.509 ± 0.283	0.0150	0.18
Fluo	18	354.6 ± 14.2	4.38	0.027 ± 0.0074	0.0324 ± 0.0089	$-2.06 \times 10^{-4} \pm 2.25 \times 10^{-5}$	2.619 ± 0.132	0.0124	0.19
Phen	53	1224 ± 35.4	4.91	0.037 ± 0.0104	0.0433 ± 0.0122	$-2.37 \times 10^{-4} \pm 2.23 \times 10^{-5}$	2.573 ± 0.078	0.0510	0.27
Pyre	18	5914 ± 281.5	5.60	0.042 ± 0.0109	0.0533 ± 0.0139	$-2.08 \times 10^{-4} \pm 6.50 \times 10^{-5}$	2.701 ± 0.054	0.0052	0.30

[a] N = number of observations. [b] K_{oc}, soil organic carbon normalized partitioning coefficient (mL/g). [c] MWSE as defined in Table 2; here, $\nu = N - 4$. [d] Packing efficiency (η_p) is defined as the ratio of solid Q_o' to the adsorbed liquid Q_o' assumed for Figure 6a (0.141 cm^3/kg). [e] Mean ± standard deviation.

calculated fraction of sorption that can be attributed to the adsorption component for all nine chemicals, plotted as a function of relative equilibrium concentration. These results thus explain why more apparent isotherm nonlinearity (lower Freundlich isotherm exponent) was observed for the more hydrophobic chemicals.

Fractional Contribution of Adsorption. Despite the low values of fitted Freundlich exponents, our adsorption-partitioning modeling results reflect a dominance of the partitioning phenomenon for all chemicals at sufficiently high relative aqueous concentration. More specifically, Figure 4 illustrates that, at C_e/S_w values above roughly 0.1, the fractional contribution of adsorption is less than 0.40 for all nine chemicals. Moreover, the adsorption capacity becomes saturated at roughly similar relative concentration for all nine chemicals. The relative concentration at which the adsorption capacity equals 50% of Q_{max} can be simply estimated as $(1/b)/S_w$ and is shown in the right-most column of Table 3. This value is in the range of 0.008 to 0.079 for all chemicals, with an average of 0.032 (±0.021, one SD). For all compounds except naphthalene, phenanthrene, and pyrene, these relative concentrations are higher than the values of 0.010−0.015 for apparent saturation $(C_e/S_w)_{as}$ that were observed by Chiou and Kile (*9*) for trichloroethene and ethylene dibromide on a peat soil.

Composite Adsorption-Partitioning with Polanyi−Manes Modeling Approach. For application of the Polanyi−Manes approach, eq 6 was used to fit the observed sorption data. For the purposes of such calculations, the molar volume is commonly estimated as the ratio of molecular weight and the density of the chemical in its pure form (*30*). The molar volumes and solubility values used for the calculation of adsorption potential density are as given in Table 1.

The fitted parameters K_p (ml/g), Q_o' (cm^3/kg soil), a', and b' for all chemicals along with the calculated errors are summarized in Table 4. Figure 5 shows the experimental data and the model simulations in an identical manner as Figure 2. As with the Langmuir-type approach, the total sorption data and the adsorption component can be successfully modeled by the Polanyi-based adsorption-partitioning model for all chemicals. This is expected since the Polanyi-based isotherm shape is similar to that of Langmuir-type isotherm in having an adsorption plateau at very high relative concentrations. As before, the statistical comparison of goodness of model fit yields ambiguous results—MSWE values have both lower and higher values, relative to either the Langmuir or Freundlich models.

Plots of adsorbed volume per mass of soil against the adsorption potential density for all chemicals are shown in Figure 6 (parts a (liquid chemicals) and b (solid chemicals)). As the Polanyi-based model would predict, the adsorbed volumes of liquid chemicals fall essentially on a single line

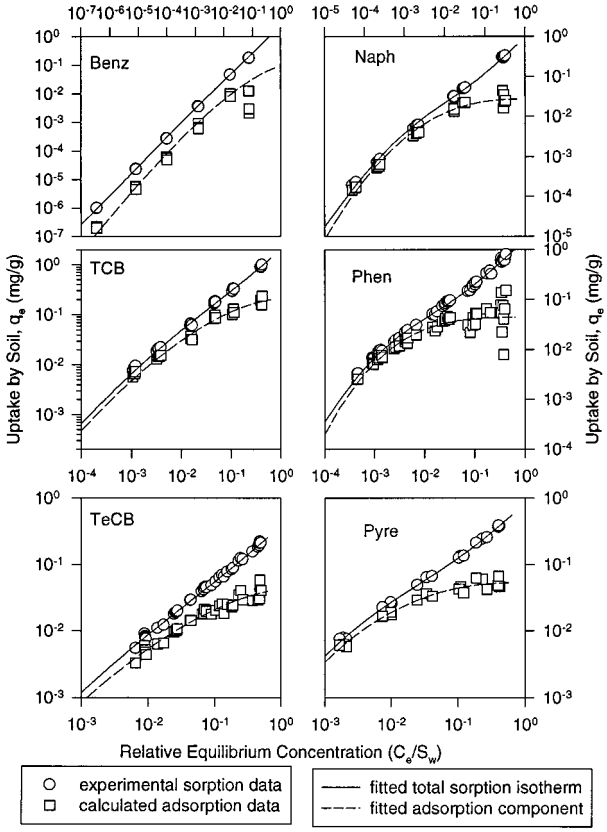

FIGURE 5. Representative composite adsorption-partitioning isotherms with Polanyi-based isotherm for adsorption component.

(Figure 6a) and with a common value of adsorption capacity (0.141 cm^3/kg soil) for all liquid chemicals tested. In contrast, the adsorption capacities for solid chemicals (Figure 6b) are lower, in the range of 0.022−0.042 cm^3/kg soil. These results are qualitatively in accord with the aforementioned observations of adsorption on activated carbon, where solid-phase adsorbates were reported to pack less efficiently (*25, 26, 30*). If we define the packing efficiency (η_p) as the adsorption capacity of a solid relative to that of any liquid (0.141 cm^3/kg), the calculated values are in the range of 0.16−0.30, as shown in the right-most column of Table 4. These estimates are much lower than the average efficiency of approximately 0.77 observed for the adsorption of solid sorbates from water by activated carbon (*26, 30*). However, we re-emphasize that our experiments were not able to provide a sensitive measure of maximum adsorption capacity, owing to a dominance of the partitioning component of sorption at the associated aqueous concentration.

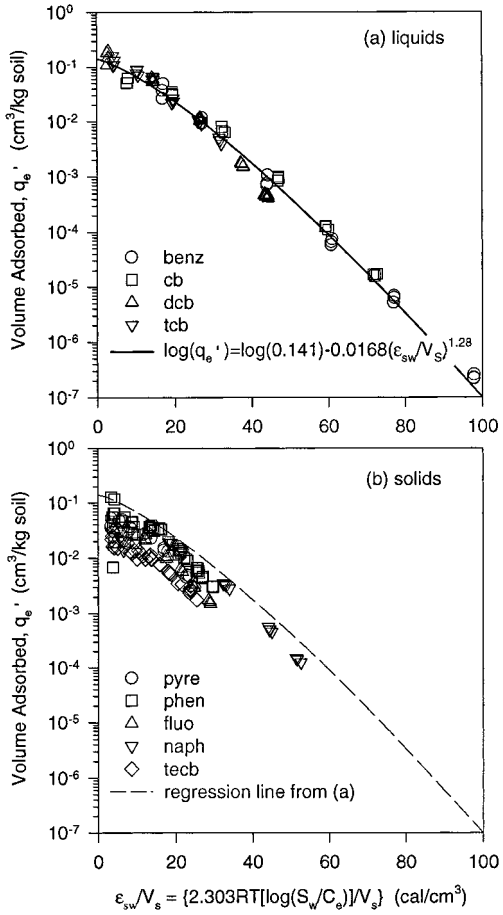

FIGURE 6. Polanyi-based adsorption isotherms for nine organic chemicals plotted as adsorbed volume versus adsorption potential density: (a) chemicals that are liquids at 22 °C and (b) chemicals that are solids at 22 °C.

If the subcooled liquid solubility of a solid is used for calculation of adsorption potential, the data of Figure 6b will all move to the right and become more coincident with the data for liquid compounds. However, the data still plateau at the value of the previously estimated maximum adsorbed volume, and model fitting (results not shown) gives similar values of packing efficiency. Moreover, adsorption as a subcooled liquid is difficult to justify in light of both the prior work with activated carbon (*25*, *26*, *30*) and the high heats of fusion (ΔH_f) of the sorbates. More specifically, ΔH_f values for the five chemicals in question range from 5 to 7 kcal/mol (*43*) and are well in excess of the energy differences between adsorption as a solid and adsorption as a liquid. The latter are calculated as $2.3RT \log(S_{w,subcooled}/S_{w,solid})$ and range between 0.7 and 1.4 kcal/mol for these chemicals (*43*). The heats of fusion are also greater than absolute energies of adsorption (ϵ_{sw}), which were always below 5 kcal/mol and are on the order of 0.5 kcal/mol at the high concentrations where Q_o' is estimated. Thus, pore-filling as a solid adsorbate is a reasonable a priori assumption.

Together, the isotherm results of Figure 6a,b provide strong evidence that Polanyi modeling assumptions hold and that adsorption uptake may indeed be the result of solute condensation into micropores that have a comparatively low affinity for water. The coincident adsorption isotherm of liquid chemicals shown in Figure 6a allows all results to be explained without inferring any difference in adsorption process between relatively small and large molecules. The reduced maximum adsorption capacity for solid chemicals (shown in Figure 6b) is similar to previous observations for activated carbon and can presumably be attributed to similar causes—i.e., to differences in packing efficiency within micropores.

Overall, the observed adsorption results with Dover aquitard material agree well with expectations of an adsorption-partitioning model that assumes adsorption by pore-filling. Although both Langmuir-type and Polanyi-based models were successful in simulating the adsorption data, we are encouraged by the single correlation exhibited in Figure 6a and believe that pore filling within HSACM may be a plausible mechanistic explanation of our data. We have further verified the applicability of this modeling approach with other geosorbents and through additional investigations under conditions of competitive uptake in binary systems (*40*). These results are in preparation for future publication.

Acknowledgments

This research was supported by the Air Force Civil Engineering Support Agency under the auspices of the U.S. Army Research Office Scientific Service Program administered by Battelle (Contract No. DAAL03-91-C-0034), the National Science Foundation (Presidential Young Investigator Award BES-9296241), and a Dupont Educational Aid Grant. We are particularly grateful to Prof. Milton Manes (Kent State University) for valuable discussions regarding the application of Polanyi adsorption theory to our data and Dr. Cary T. Chiou (U.S. Geological Survey) for many valuable suggestions and comments.

Literature Cited

(1) Karickhoff, S. W.; Brown, D. S.; Scott, T. A. *Water Res.* **1979**, *13*, 241−248.
(2) Karickhoff, S. W. *Chemosphere* **1981**, *10*, 833−846.
(3) Chiou, C. T.; Peters, L. J.; Freed, V. H. *Science* **1979**, *206*, 831−832.
(4) Chiou, C. T.; Porter, P. E.; Schmedding, D. W. *Environ. Sci. Technol.* **1983**, *17*, 227−231.
(5) Means, J. C.; Wood, S. G.; Hassett, J. J.; Banwart, W. L. *Environ. Sci. Technol.* **1980**, *14*, 1524−1529.
(6) Schwarzenbach, R. P.; Westall, J. C. *Environ. Sci. Technol.* **1981**, *15*, 1360−1367.
(7) Weber, W. J., Jr.; McGinley, P. M.; Katz, L. E. *Environ. Sci. Technol.* **1992**, *26*, 1955−1962.
(8) Weber, W. J., Jr.; Huang, W. *Environ. Sci. Technol.* **1996**, *30*, 881−888.
(9) Chiou, C. T.; Kile, D. E. *Environ. Sci. Technol.* **1998**, *32*, 338−343.
(10) Xing, B.; Pignatello, J. J. *Environ. Sci. Technol.* **1997**, *31*, 792−799.
(11) Pignatello, J. J.; Xing, B. *Environ. Sci. Technol.* **1996**, *30*, 1−11.
(12) Luthy, R. G.; Aiken, G. R.; Brusseau, M. L.; Cunningham, S. D.; Gschwend, P. M.; Pignatello, J. J.; Reinhard, M.; Traina, S. J.; Weber, W. J., Jr.; Westall, J. C. *Environ. Sci. Technol.* **1998**, *31*, 33341-3347.
(13) Huang, W.; Young, T. M.; Schlautman, M. A.; Yu, H.; Weber, W. J., Jr. *Environ. Sci. Technol.* **1997**, *31*, 1703−1710.
(14) Feng, L.; Han, S.; Wang, L.; Zhang, Z. *Chemosphere* **1996**, *33*, 2113-2120.
(15) Adamson, A. W. *Physical Chemistry of Surfaces*; John Wiley & Sons: New York, 1982.
(16) Xing, B.; Pignatello, J. J.; Gigliotti, B. *Environ. Sci. Technol.* **1996**, *30*, 2432−2440.
(17) Xing, B.; Pignatello, J. J. *Environ. Sci. Technol.* **1997**, *31*, 1578−1579.
(18) Graber, E. R.; Borisover, M. D. *Environ. Sci. Technol.* **1998**, *32*, 258−263.
(19) Borisover, M. D.; Graber, E. R. *Environ. Sci. Technol.* **1997**, *31*, 1577.
(20) Gustafesson, O.; Gschwend, P. M. *Geochim. Cosmochim. Acta* **1998**, *62*, 465.
(21) Goldberg, E. D. *Black Carbon in the Environment*; John Wiley & Sons: New York, 1985.
(22) Derenne, S.; Largeau, C.; Casadevall, E.; Berkaloff, C.; Rousseau, B. *Geochim. Cosmochim. Acta* **1991**, *55*, 1041−1050.
(23) Manes, M.; Hofer, L. J. E. *J. Phys. Chem.* **1969**, *73*, 584−590.
(24) Wohleber, D. A.; Manes, M. *J. Phys. Chem.* **1971**, *75*, 61−64.

(25) Chiou, C. T.; Manes, M. *J. Phys. Chem.* **1973**, *77*, 809−813.
(26) Chiou, C. T.; Manes, M. *J. Phys. Chem.* **1974**, *78*, 622−626.
(27) Rosene, M. R.; Ozcan, M.; Manes, M. *J. Phys. Chem.* **1976**, *80*, 2586.
(28) Greenbank, M.; Manes, M. *J. Phys. Chem.* **1981**, *85*, 3050−3059.
(29) Greenbank, M.; Manes, M. *J. Phys. Chem.* **1982**, *86*, 4216−4221.
(30) Manes, M. Activated Carbon Adsorption Fundamentals. In *Encyclopedia of Environmental Analysis and Remediation*; Meyers, R. A., Ed.; John Wiley: New York, 1998; pp 26−68.
(31) Hansen, R. S.; Fackler, W. V., Jr. *J. Phys. Chem.* **1953**, *57*, 634−637.
(32) Reucroft, P. J.; Simpson, W. H.; Jonas, L. A. *J. Phys. Chem.* **1971**, *75*, 3526−3531.
(33) Crittenden, J. C.; Hand, D. W.; Arora, H.; Lykins, B. W., Jr. *J. Am. Water Works Assoc.* **1987**, *79*, 74−82.
(34) Wohleber, D. A.; Manes, M. *J. Phys. Chem.* **1971**, *75*, 3720−3723.
(35) Dubinin, M. M. *Chem. Rev.* **1960**, *60*, 235−241.
(36) Ramsey, K. W. *Geologic Map of the Miflord and Mispillion River Quadrangles*; Geologic Map Series No. 8; Delaware Geological Survey: Newark, DE, 1993.
(37) Ball, W. P.; Xia, G.; Durfee, D. P.; Wilson, R.; Brown, M.; Mackay, D. M. *Ground Water Monit. Rem.* **1997**, *17*, 104−121.
(38) Klute, A. *Methods of Soil Analysis: Part 1. Physical and Mineralogical Methods*, 2nd ed.; Klute, A., Ed.; American Society of Agronomy, Soil Science Society of America: Madison, 1986; p 1188.
(39) Ball, W. P.; Roberts, P. V. *Environ. Sci. Technol.* **1991**, *25*, 1223−1237.
(40) Xia, G. *Sorption Behavior of Nonpolar Organic Chemicals on Natural Sorbents;* Ph.D. Dissertation, The Johns Hopkins University: Baltimore, MD, 1998; p 297.
(41) Chiou, C. T.; McGroddy, S. E.; Kile, D. E. *Environ. Sci. Technol.* **1998**, *32*, 264−269.
(42) Kile, D. E.; Chiou, C. T.; Zhou, H.; Li, H.; Xu, O. *Environ. Sci. Technol.* **1995**, *29*, 1401−4106.
(43) Schwarzenbach, R. P.; Gschwend, P. M.; Imboden, D. M. *Environmental Organic Chemistry*; Wiley-Interscience: New York, NY, 1993.
(44) Mackay, D.; Shiu, W.; Ma, K. *Illustrated Handbook of Physical-Chemical Properties and Environmental Fate for Organic Chemicals*; Lewis Publishers: Chelsea, MI, 1992.
(45) Suntio, L. R.; Shiu, W. Y.; Mackay, D. *Chemosphere* **1988**, *17*, 1249−1290.

Received for review April 23, 1998. Revised manuscript received October 23, 1998. Accepted October 26, 1998.

ES980581G